Progress In Electromagnetics Research B, Vol. 38, 315–331, 2012

A MONOPOLE MICROSTRIP ANTENNA WITH ENHANCED DUAL BAND REJECTION FOR UWB APPLICATIONS

P. Tilanthe[1,*], P. C. Sharma[2], and T. K. Bandopadhyay[3]

[1]Department of EC, TRUBA College of Engineering and Technology, Indore, India

[2]Department of ECE, S. D. Bansal College of Technology, Indore, India

[3]Department of ECE, Bansal Institute of Science and Technology, Bhopal, India

Abstract—In this paper, a compact, planar ultrawideband (UWB) monopole microstrip antenna is proposed which offers dual band notch characteristics with enhanced rejection at frequency bands centered at 3.4 GHz and 5.5 GHz. To realize enhanced band notched characteristics at 3.4 GHz, a pair of filters is incorporated which includes an inverted 'L' shaped slot and a twisted 'J' shaped slot in the patch element. Another pair of filters comprises of a spur line filter in the feed line and 'U' shaped slot in the patch are used to get a strong frequency band rejection centered at 5.5 GHz. Step by step development of the antenna with its analysis in frequency and time domain is presented. The prototype is fabricated and the measured results are presented which are in close similarity to the simulated results.

1. INTRODUCTION

The UWB antenna is an important component in the UWB system as it acts as a filter which only passes the desired frequency components designated by the FCC [1]. UWB digital communication systems which uses an extremely wide frequency range are meant for providing radio communication at low power with high bit rates [1–5]. The performance of the UWB antennas in both time and frequency domain are of equally importance which makes the UWB antenna design a challenging and interesting field of research [6–14]. An

Received 24 December 2011, Accepted 1 February 2012, Scheduled 9 February 2012

* Corresponding author: Pramendra Tilanthe (pramendra20@yahoo.com).

excellent UWB antenna is one which can transmit and receive the frequencies over the bandwidth designated by FCC [1, 2]. The antenna must also possess stable radiation characteristics and gain over the operating UWB band. The antenna's pulse preserving capabilities for the transmission and reception of the ultra-narrow pulse is investigated in the time domain. Two of the most important time domain properties of UWB antenna are fidelity/correlation factor and symmetry/pulse width stretch ratio [15, 16]. The fidelity is defined as maximum normalized cross-correlation of the incident voltage and the electric field in the far field region. The symmetry is a measure of the symmetry of the waveform in the far field region. The other important characteristics are transfer function/impulse response and group delay [17]. Apart from the frequency and time domain characteristics mentioned above, a compact/low profile antenna size is desirable for integration requirement with UWB system.

The UWB antenna design comprise of some other challenges too. Some portions of the UWB bandwidth (which is designated by FCC) are shared by other existing narrowband services also. One of the services is wireless local area network (WLAN) IEEE802.11a and HIPERLAN/2 WLAN operating in 5–6 GHz band. Another service named as Worldwide Interoperability for Microwave Access (WiMAX) which utilizes a frequency band 3.3 GHz–3.6 GHz is used in some European and Asian countries. For some UWB applications which does not require overall compact size of the transmitter or receiver, appropriately designed band pass filters or spatial filter such as a frequency selective surface (FSS) above the antenna can be used to suppress the dispensable bands [18]. However for the UWB systems which demand a compact, less complex and low cost design, frequency band rejection function may be employed in the antenna itself, which includes embedding optimal shaped slot in the radiating patch or in the ground plane. The frequency band notch characteristics can be essentially achieved using one of the two methods [29]. The first group of methods includes adding a perturbation in the surface current flowing in the antennas radiating elements. The second class of methods employs adding a perturbation on the antenna feed line or in the ground plane. Some of the recent examples includes embedding an H shaped slot in radiating patch [19], arc shaped slot [20] and a pair of inverted L and U shaped slot in radiating element and a square shaped slot in ground plane [21]. A few good examples of UWB antennas may also be found in [22–26].

In this paper, a compact, microstrip fed, monopole UWB antenna with dual notched characteristics is presented. This work adds perturbation in the surface current density of the radiating element

and the feed element. Initially a reference antenna is designed, which exhibits radiating characteristics in the frequency band 3–11 GHz. By etching an inverted 'L' shaped slot in the radiating patch, a single band frequency notch is created at 3.4 GHz. Enhanced rejection at 3.4 GHz is obtained by carving another tilted 'J' shaped slot from the opposite side of the radiating element. In order to achieve non-radiating characteristics at 5.5 GHz a spur line filter is incorporated in the microstrip feed line. Another 'U' shaped slot is optimally cut from the radiating patch to get enhanced rejection at the same frequency band. Finally, the antenna with all four filtering components is optimized and fabricated, and the characteristics are measured. A good match is observed in the simulated and measured characteristics. The frequency domain analysis only tells about the influence of applied method on the frequency band notch, radiation pattern, gain, etc. However, the time domain analysis is also important to estimate the influence on the pulse preserving properties, stretch ratio, ringing etc. Therefore, the antenna is also analyzed on the basis of the time domain characteristics to investigate its employability in the practical UWB systems. It is found that the antenna exhibits fairly good stretch ratio and correlation factor. Apart from these properties, the proposed antenna exhibits an almost stable omnidirectional radiation pattern and a reasonably good gain over the operating UWB band.

2. ANTENNA DESIGN

The geometry of the reference antenna is presented in Figure 1. The antenna is printed on FR-4 substrate of thickness 1.59 mm and a

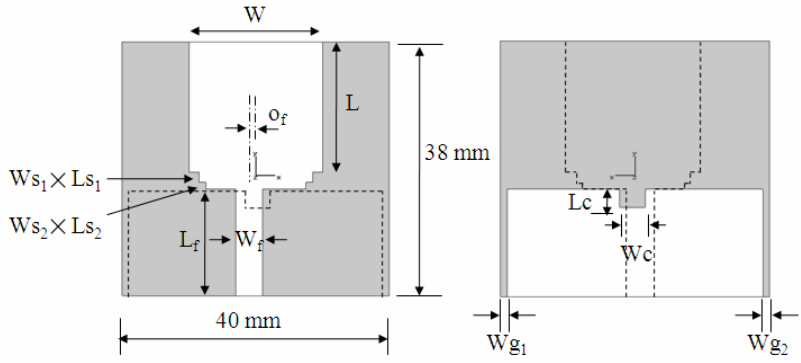

Figure 1. Configuration of the reference antenna.

Table 1. Details of reference antenna's parameters.

Antenna Component	Symbols and their values for the proposed antenna (in mm)
Patch	$W = 20$, $L = 19.5$
Feed	$W_f = 4$, $L_f = 16$
Steps at patch bottom	$W_{s1} = 1.5$, $L_{s1} = 1.5$, $W_{s2} = 1$, $L_{s2} = 1$
Ground Slot	$W_c = 3.8$, $L_c = 2.7$, $W_{g1} = 1$, $W_{g2} = 1$, $O_f = 1.5$
Substrate	Width = 40, Length = 38

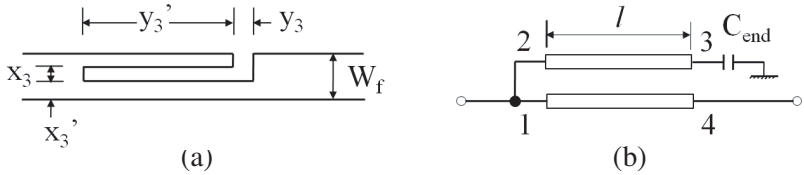

Figure 2. (a) Spur-line filter embedded in microstrip line, (b) coupled pair transmission line equivalent.

relative dielectric constant (ε_r) of 4.4. The patch having dimension $W \times L$ is excited using a 50 Ohm microstrip line. The ground plane is modified to achieve a better impedance matching. The ground plane area is reduced by removing the metal which is present beneath the patch. Also the rectangular slot is optimally cut from the ground plane with the dimension $L_c \times W_c$ to get wide band impedance matching. The details of the parameters of this reference antenna are given in Table 1.

The modification in the reference antenna includes cutting an inverted 'L' shaped slot (referred to as filter-1 in this communication), shown in Figure 3(a). Another slot of twisted 'J' shape is cut (referred to as filter-2) from the opposite side of the radiating element as shown in Figure 3(b). These two slots are optimally embedded to attain a frequency notch characteristic centered at 3.4 GHz. The length of the two slots etched in the patch can be deduced as in Equations (1) and (2). The two slots act as two quarter wave length resonators.

The total length of the inverted "L" shaped slot (L_1) is 11.6 mm whereas the total length of the twisted 'J' shaped slot (L_2) is 12.2 mm. The width of the two slots and their vertical location on the radiating patch are optimized to get the desired frequency notch (which is

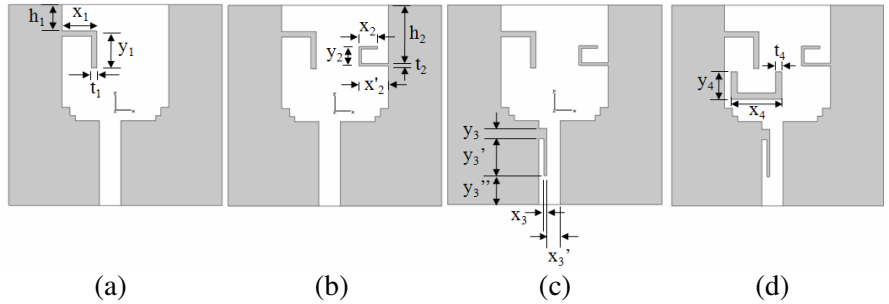

Figure 3. Evaluation of the proposed antenna showing dimension of (a) filter-1, (b) filter-2, (c) filter-3 and (d) filter-4.

3.4 GHz).

$$(x_1 + y_1 - t_1) = L_1 \approx \frac{c}{4f_{\text{notch}}\sqrt{\varepsilon_{eff}}} \tag{1}$$

$$(x_2 + x_2' + y_2 - 2t_2) = L_2 \approx \frac{c}{4f_{\text{notch}}\sqrt{\varepsilon_{eff}}} \tag{2}$$

where

$$\varepsilon_{eff} = \frac{\varepsilon_r + 1}{2} \tag{3}$$

f_{notch} is the notch frequency, c is the speed of light, ε_r is the dielectric constant of substrate.

A spur line filter (referred to as filter-3) is added in the microstrip feed line as shown in Figure 3(c). The spur line filter consists of a coupled pair of quarter wave length (calculated at the notch frequency) long microstrip lines [27]. It consists of an open circuit at the end of one of the coupled lines and with both lines connected together at the other end. The equivalent configuration of spur-line filter comprise of a four port coupled line network as shown in Figure 2. Out of the four ports, one is terminated in a capacitance which represents the discontinuity capacitance. The length of spur (designated as y_3' in Figure 3(c)) and the gap (designated as y_3 in Figure 3(c)) determines the notch frequency (which is 5.5 GHz).

$$y_3 + y_3' = \frac{c}{4f_{\text{notch}}\sqrt{\varepsilon_{eff}}} \tag{4}$$

Finally, a 'U' shaped slot is cut (referred to as filter-4) and optimized, as shown in Figure 3(d) to get an enhanced rejection in the frequency band 5.15–5.85 GHz. The dimensional parameters of all the four filters are given in Table 2. The fabricated prototype is shown in Figure 4. The asymmetric microstrip line does not have any

Table 2. Optimized values of all filter's parameters.

Filter	Symbols and their values (in mm)
Filter-1	$x_1 = 6.5$, $y_1 = 5.5$, $h_1 = 5$, $t_1 = 0.4$
Filter-2	$x_2 = 3.5$, $x_2' = 5.5$, $y_2 = 3.6$, $h_2 = 11.3$, $t_2 = 0.2$
Filter-3	$x_3 = 0.2$, $x_3' = 3.55$, $y_3 = 1$, $y_3' = 7$, $y_3'' = 5.5$
Filter-4	$x_4 = 9.6$, $y_4 = 5.2$, $t_4 = 1.2$

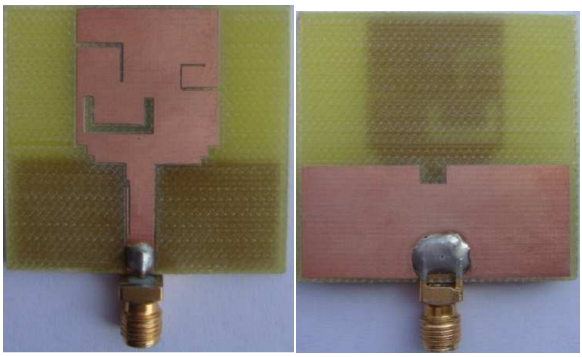

(a) (b)

Figure 4. Fabricated prototype. (a) Front, (b) back view.

significant effect on the performance of the reference antenna but plays a very important role, once all the four filters have been embedded. The asymmetric placement of feed line not only gives rise to a fairly good impedance mismatch in the frequency band 5.15–5.85 GHz, but also provides an impedance match at higher frequencies. The position of feed line, which contains spur-line filter too, is optimized. It is also observed that a symmetric feed line gives an impedance mismatch to the entire frequency band of 5–6 GHz.

3. FREQUENCY DOMAIN RESULTS

The reference antenna (shown in Figure 1) is simulated in the frequency band 2–11 GHz to investigate its radiation characteristics.

For the simulation, the full wave EM solver CST microwave studio is used [28], based on the finite integration technique method. The parameters of the reference antenna are optimized to get a VSWR < 2 and stable radiation characteristics throughout the frequency band

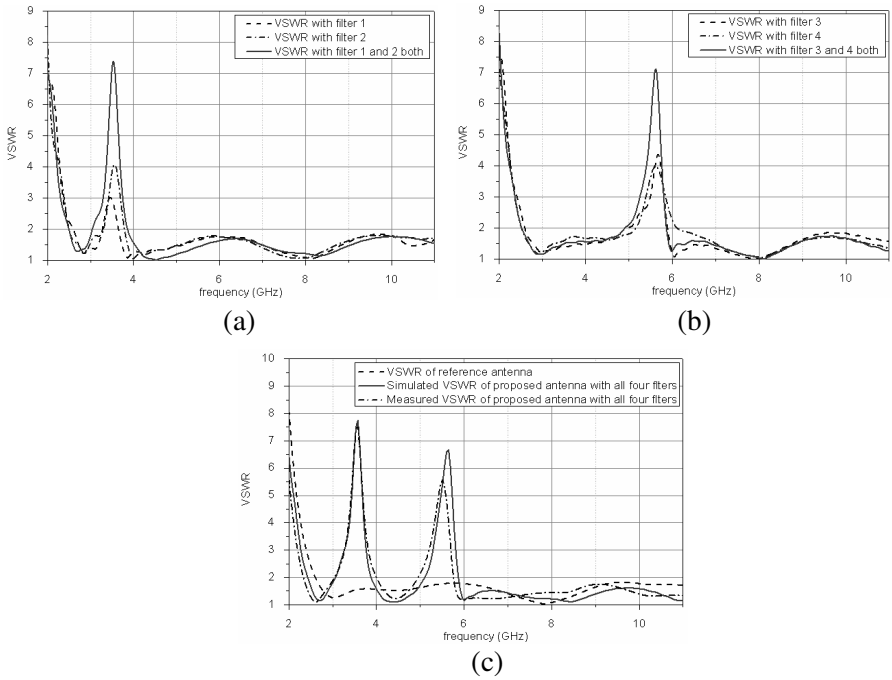

Figure 5. VSWR characteristics (a), (b) when embedded with individual filters and their combination, (c) comparison of proposed antenna (with all four filters) with that of the reference antenna.

3 GHz–10.6 GHz as shown in Figure 5(c), which fulfills the FCC criterion. The VSWR characteristics after embedding with filter-1 and filter-2 in the reference antenna (individual and their combination) are shown in Figure 5(a). When the filter-1 is added (though the inverted 'L' shaped slot is cut) to the antenna, it shows an impedance mismatch in the frequency band 3.2 GHz–3.6 GHz as the VSWR > 2 in this band. However, the maximum VSWR is only 3 (which is just sufficient but not good) at the center frequency of the band which is 3.45 GHz. To improve the rejection in this band, filter-2 is added to the antenna. The characteristic of the antenna with added filter-2 alone is also separately investigated. As observed from Figure 5(a), in this case the antenna exhibits frequency rejection in the frequency band 3.3 GHz–3.7 GHz, with a peak VSWR of 4.1. When filter-1 and filter-2 are simultaneously added to the antenna, the frequency rejection is improved in the WiMAX frequency band by exhibiting a maximum VSWR of 7.4 and with a minimum influence on the remaining band.

The VSWR characteristics with added filter-3 alone and filter-

4 alone in the reference antenna are shown in Figure 5(b). When spur line filter (filter-3 which is designed at 5.4 GHz) is added to the reference antenna, it shows a 5.1–5.89 GHz band rejection. To enhance the frequency rejection capability of the reference antenna in this band, another filter ('U' shaped slot) is added to this. The effect of addition of both the filters gives rise to the improvement in the frequency rejection capability of the antenna in the WLAN frequency band, as observed from Figure 5(b).

After adding all the four filters simultaneously to the reference antenna, it shows an enhanced dual band frequency rejection as observed from Figure 5(c). Comparison of the VSWR characteristics of the simulated results and measured results of the proposed antenna is also shown in Figure 5(c). A good compromise is observed between the measured and simulated results. A slight upward frequency shift is observed in the frequency band centered at 5.4 GHz in the measured results which can be understood due to the following two reasons. The effect of soldering is not taken into account in the simulation. The loss tangent of the substrate is kept 0.02 during simulation of the antenna which is actually a function of the frequency.

The measured radiation patterns of the proposed antenna in two principle planes are shown in Figure 6. The E plane pattern (which contains the YOZ plane) at three operating frequencies of the UWB band are given in Figure 6(a).

As observed, the pattern is almost stable throughout the UWB band, an important requirement from system design point of view. The H plane pattern (XOZ plane) is shown in Figure 6(b) which is

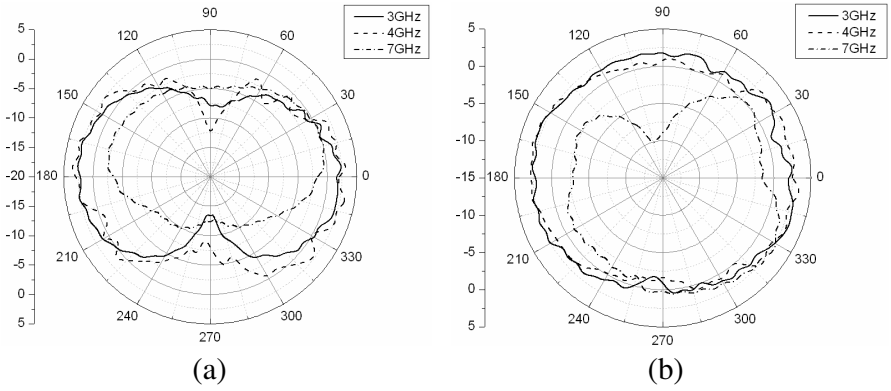

Figure 6. Measured radiation pattern of the proposed antenna. (a) E plane (YOZ) pattern and (b) H plane (XOZ) pattern.

mostly omnidirectional throughout the frequency band.

The comparison of the gains of the proposed antenna with that of the reference antenna is shown in Figure 7. As observed, the reference antenna has a gain variation between 2.9 dB and 6 dB in the UWB frequency band. The gain of the proposed antenna almost follows the gain of the reference antennas over the UWB frequency band, except the two notch bands. In the first notch band, the gain dips down by 3.5 dB, while in the second notch band, it dips down by 5.2 dB

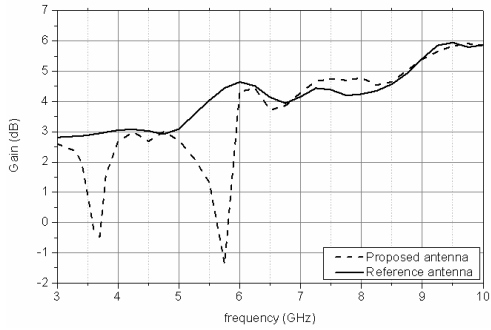

Figure 7. Comparison of the gain of the proposed antenna and the reference antenna.

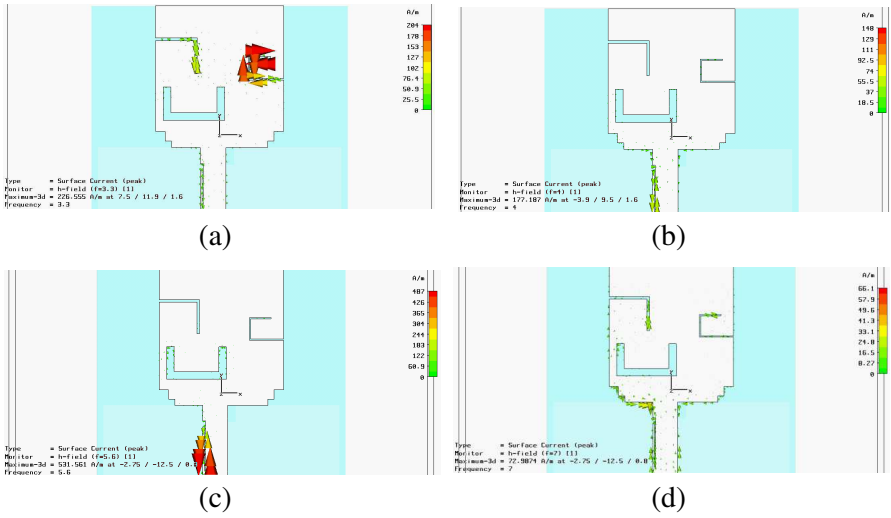

Figure 8. Surface current density at (a) 3.3 GHz, (b) 4 GHz, (c) 5.5 GHz, (d) 7 GHz.

as compared to the reference antenna with minimum influence on the remaining band.

The surface current distribution analysis of the proposed antenna in the UWB band is shown in Figure 8 at frequencies 3.3 GHz, 4 GHz, 5.5 GHz and 7 GHz. It is observed from Figure 8(a) that in the first notch band (3.3 GHz–3.6 GHz) the surface current is mainly distributed across the filter-1 and filter-2 as compared with the other parts of the radiator. The effect of the perturbation due to filter-1 and filter-2 is to create a destructive interference between the forward and reverse traveling currents which makes the antenna non-responsive in the WiMAX frequency band. This frequency band can be tuned by changing the dimensions and position of the two filters. It is observed that filter-2 has more influence on the notch frequency than filter-1. As observed from Figure 8(c), the current is distributed mainly along the spur-line filter and a little bit around the 'U' slot at 5.5 GHz which is the center frequency of the WLAN frequency band. The spur line filter acts as band stop filter whose stop band is the unwanted WLAN frequency band. The dimensions of the spur line filter can be properly controlled to get the frequency rejection characteristics in the desired frequency band. From the current distribution analysis, it is found that the spur-line filter dominates over 'U' slot filter to control the notch characteristics. Apart from the notch frequency bands, at 4 GHz and 7 GHz, which are the radiating frequencies, the surface current flows through the microstrip feed line and radiating element and is not concentrated at any specific filter. Thus it may be concluded that the radiating frequency bands are unaffected by the filters.

The analysis of the transmission for the reference antenna and the proposed antenna between two identical antennas is done. The

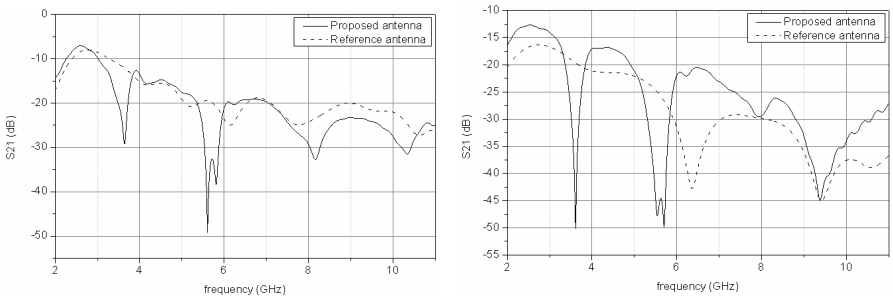

Figure 9. Transmission coefficient (S_{21}) between similar antennas with distance 300 mm in (a) face to face configuration, (b) side by side configuration.

investigation is done in two orientations: face to face and side by side as shown in Figure 9. It can be seen from Figure 9(a) that for face to face orientation (at 3.4 GHz), the value of S_{21} goes down to -29 dB which is -11 dB for the reference antenna. Thus a decrease of 18 dB is obtained in the system transfer parameter due to addition of filter-1 and filter-2. Similarly for the same orientation, the system transfer parameter shows an average dip of -20 dB in the WLAN frequency band. In the un-notched frequency band, the system transfer functions for the reference antenna and proposed antenna are almost identical. Similar dips at corresponding notch frequencies are observed in the system transfer function of the proposed antenna for side by side orientation from Figure 9(b).

4. PULSE PRESERVING PERFORMANCE OF PROPOSED ANTENNA

The UWB systems are such systems which have a bandwidth requirement greater than 500 MHz. UWB signals are pulse based waveforms compressed in time, instead of sinusoidal waveforms compressed in frequency. Since UWB systems use pulse transmission, it is important to investigate how much the antenna is distorting the pulse. Two time domain parameters, namely correlation factor and stretch ratio, are considered for investigation of the pulse preserving performance of the proposed antenna. The pulse distortion during transmission and reception is mainly caused by the bandwidth mismatch between the UWB antenna and the input source pulse. A UWB signal (the 5th derivative of the Gaussian pulse) is considered [30–32], which is a single pulse with the most effective spectrum under the FCC limitation floor [33].

$$S_1(t) = GM_5(t) = A\left(-\frac{t^5}{\sqrt{2\pi}\sigma^{11}} + \frac{10t^3}{\sqrt{2\pi}\sigma^9} - \frac{15t}{\sqrt{2\pi}\sigma^7}\right)\exp\left(-\frac{t^2}{2\sigma^2}\right) \quad (5)$$

where C is a constant which can be chosen to comply with peak power spectral density that the FCC suggests, and σ has to be 51 ps to ensure that the shape of the spectrum complies with the FCC spectral mask.

To determine the correlation factor, a channel is considered with the time domain pulse $S_1(t)$ as input signal (shown in Figure 10) and the theta component of the electric field intensity in the far field as the output signal. During CST simulations, the proposed antenna is set to transmit this pulse, and three virtual probes are placed in the far field at $\theta = 0°$, $45°$ and $90°$ in order to monitor the theta component of electric field intensity. The corresponding E_θ components of electric field intensity (designated as $S_2(t)$) as seen by the virtual probes for these three cases are given in Figure 11.

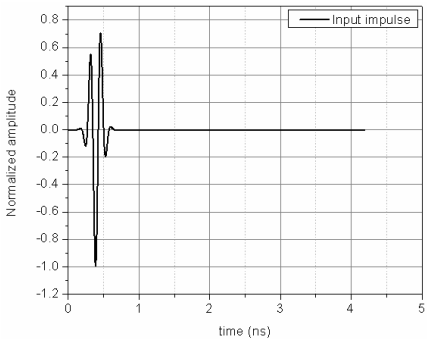

Figure 10. Transmitting antennas input.

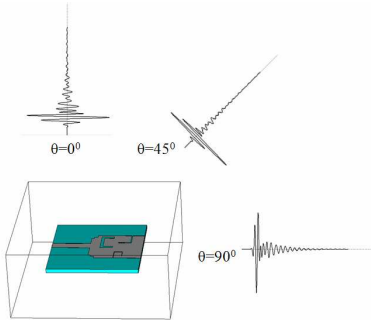

Figure 11. The received far field signals by virtual probes for $\varphi = 90°$ and varying θ in the E plane.

Table 3. Correlation factors for the proposed antenna between the input pulse and the signal received in far field for different probe positions.

Location of probe	Correlation factor ρ
$\theta = 0°$, $\varphi = 90°$	0.8389
$\theta = 45°$, $\varphi = 90°$	0.9227
$\theta = 90°$, $\varphi = 90°$	0.8749

The correlation factor is calculated between $S_1(t)$ and $S_2(t)$ to evaluate the pulse preserving capability of the proposed antenna by using Equation (6).

$$\rho = \max_{\tau} \left\{ \frac{\int s_1(t) s_2(t-\tau) dt}{\sqrt{\int s_1^2(t) dt} \sqrt{\int s_2^2(t) dt}} \right\} \tag{6}$$

where τ is delay which is varied to make ρ in (6) a maximum. For the proposed antenna, the correlation factors between the transmitted pulse and received signal are summarized in Table 3.

As observed from Figure 11 and Table 3, the ringing is the lowest, and correlation factor is maximum for $\theta = 45°$, $\varphi = 90°$ as compared with the two other cases. In the received signal, pulse distortion and ringing is observed, which may be due to the finite energy storage effects of the substrate. A detailed study of the energy storage effect of the substrate on the ringing and distortion may be found in [34].

In the UWB systems, the transmitted pulse broadening is an

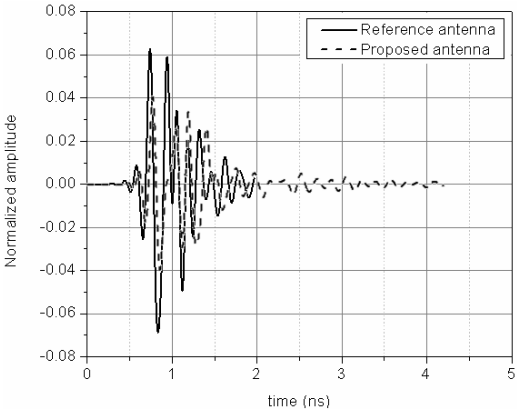

Figure 12. Received output from the proposed and reference antennas in receiving mode.

important parameter. If the broadening of the transmitted pulse is minimum, then more pulse train in shorter gap may be transmitted in a given time window resulting in a high rate of data transmission. The effective width of the received pulse may be defined as the width containing a definite percentage of the total energy [35]. For a signal $s(t)$, let the normalized cumulative energy function $E_s(t)$ be defined by Equation (7).

$$E_s(t) = \frac{\int\limits_{-\infty}^{t} |s(t')|^2 \, dt'}{\int\limits_{-\infty}^{\infty} |s(t')|^2 \, dt'} \tag{7}$$

Then after removing the first and last 5% energy portions in the time axis, the pulse width stretch ratio (SR) for 90% energy capture is given by [33] —

$$\text{SR} = \frac{E_{s_2}^{-1}(0.95) - E_{s_2}^{-1}(0.05)}{E_{s_1}^{-1}(0.95) - E_{s_1}^{-1}(0.05)} \tag{8}$$

To compute the stretch ratio, the transmit-receive antenna system is considered as a two-port network. The input pulse shown in Figure 10 is used to excite the proposed antenna/reference antenna and the same antenna arranged at a distance of 100 mm in receiving mode. The received signals for both the cases are given in Figure 12. The value of stretch ratio for the reference antenna is 2.6, and that for the proposed antenna is 3.1. For both the antennas, the energy in the

received pulse is distributed over the time window and not concentrated around the peak. The higher stretch ratio of the proposed antenna, as compared to the reference antenna, may be due to the addition of four filters in the radiating patch. These filters give rise to a perturbation in the surface current density, which leads to a destructive interference at the notched bands and results in a higher stretch ratio.

5. CONCLUSION

To minimize the potential interference between the UWB and narrowband systems, such as WiMAX and WLAN, a compact UWB antenna with enhanced dual frequency notch characteristics is proposed and discussed. Out of the four notch filters incorporated in the radiating patch, one pair, i.e., filter-1 and filter-2, provides the band notched characteristics at frequency band centered at 3.4 GHz. The other pair of filters, i.e., filter-3 and filter-4, provides the band notched characteristics at frequency 5.5 GHz. The notched bands can be controlled by adjusting the dimension and position of the slots. The frequency domain and time domain characteristics of the proposed UWB antenna have been discussed. The antenna is fabricated, and the measured results show good agreement with the simulated ones. It was observed that the ringing is difficult to reduce and that the effective pulse width is $\sim$ 1.5 ns, sufficient for data transmission at 500 Mbps. Although the proposed antenna employs four filters which makes its design complex, but that is the distinctive feature. A combination of three different methods is used: (i) perturbing the surface current density of the patch, (ii) adding spur line filter in the feed line, and (iii) defected ground plane structure. A reasonably good UWB frequency and time domain characteristics are obtained through these methods.

REFERENCES

1. FCC Report and Order for Part 15 Acceptance of Ultra Wideband (UWB) Systems from 3.1–10.6 GHz, FCC, Washington, DC, 2002.
2. First Report and Order, "Revision of part of the commissions rule regarding ultra wide band transmission system FCC02-48," Federal Communications Commission, 2002.
3. Kelly, J. R., P. S. Hall, and P. Gardner, "Band-notched UWB antenna incorporating a microstrip open-loop resonator," *IEEE Trans. Antennas Propag.*, Vol. 59, No. 8, Aug. 2011.
4. Chen, Z. N., *Antennas for Portable Devices*, Wiley, Hoboken, NJ, 2007.

5. Eldek, A. A., "Numerical analysis of a small ultra wideband microstrip-FED tap monopole antenna," *Progress In Electromagnetics Research*, Vol. 65, 59–69, 2006.
6. Liu, W.-C. and C.-F. Hsu, "CPW-FED notched monopole antenna for UMTS/IMT 2000/WLAN applications," *Journal of Electromagnetic Waves and Applications*, Vol. 21, No. 6, 841–851, 2007.
7. Naghshvarian-Jahromi, M., "Compact UWB bandnotch antenna with transmission-line-FED," *Progress In Electromagnetics Research B*, Vol. 3, 283–293, 2008.
8. Choi, N., C. Jung, J. Byun, F. J. Harackiewicz, M.-J. Park, Y.-S. Chung, T. Kim, and B. Lee, "Compact UWB antenna with I-shaped band-notch parasitic element for laptop applications," *IEEE Antennas and Wireless Propagation Letters*, Vol. 8, 2009.
9. Lizzi, L., G. Oliveri, P. Rocca, and A. Massa, "Planar monopole UWB antenna with UNII1/UNII2 WLAN-band notched characteristics," *Progress In Electromagnetics Research B*, Vol. 25, 277–292, 2010.
10. Ren, L.-S., F. Li, J.-J. Zhao, G. Zhao, and Y.-C. Jiao, "A novel compact UWB antenna with dual band-notched characteristics," *Journal of Electromagnetic Waves and Applications*, Vol. 24, Nos. 11–12, 1521–1529, 2010.
11. Zhang, G.-M., J.-S. Hong, and B.-Z. Wang, "Two novel band-notched UWB slot antennas FED by microstrip line," *Progress In Electromagnetics Research*, Vol. 78, 209–218, 2008.
12. Xie, L., Y.-C. Jiao, Y.-Q. Wei, and G. Zhao, "A compact band-notched UWB antenna optimized by a novel self-adaptive differential evolution algorithm," *Journal of Electromagnetics Waves and Applications*, Vol. 24, Nos. 17–18, 2353–2361, 2010.
13. Zhang, W.-B., Y.-C. Jiao, D.-F. Zhao, and C. Chen, "A compact band-notched slot antenna for UWB applications," *Journal of Electromagnetics Waves and Applications*, Vol. 23, No. 13, 1715–1721, 2009.
14. Lotfi Neyestanak, A. A., "Ultra wideband rose leaf microstrip patch antenna," *Progress In Electromagnetics Research*, Vol. 86, 155–168, 2008.
15. Oppermann, I., M. Hamalainen, and J. Iinatti, *UWB Theory and Applications*, John Wiley & Sons Ltd, 2004.
16. Yang, Y.-Y., Q.-X. Chu, and Z.-A. Zheng, "Time domain characterization of band notched ultrawideband antenna," *IEEE Trans. Antennas Propag.*, Vol. 57, No. 10, Oct. 2009.

17. Mohammadian, A. H., A. Rajkotia, and S. S. Soliman, "Characterization of UWB transmit-receive antenna system," *IEEE Conference on Ultra Wideband Systems and Technologies*, 2003, DOI-10.1109/UWBST.2003.1267823.
18. Yeo, J. and R. Mitra, "A novel wideband antenna package design with a compact spatial notch filter for wireless applications," *Microwave and Optical Technology Letters*, Vol. 35, 455–460, 2002.
19. Deng, J. Y., Y. Z. Yin, Q. Wang, and Q. Z. Liu, "Study on a CPW-fed UWB antenna with dual band-notched characteristic," *Journal of Electromagnetic Waves and Applications*, Vol. 23, No. 4, 513–521, 2009.
20. Xia, Y.-Q., J. Luo, and D.-J. Edwards, "Novel miniature printed monopole antenna with dual tunable band-notched characteristics for UWB applications," *Journal of Electromagnetic Waves and Applications*, Vol. 24, No. 13, 1783–1793, 2010.
21. Tilanthe, P., P. C. Sharma, and T. K. Bandopadhyay, "A compact UWB antenna with dual band rejection," *Progress In Electromagnetics Research B*, Vol. 35, 389–405, 2011.
22. Zakerl, R., C. Ghobadi, and J. Nourinia, "A modified microstrip-FED two-step tapered monopole antenna for UWB and WLAN applications," *Progress In Electromagnetics Research*, Vol. 77, 137–148, 2007.
23. Kalteh, A. A., R. Fallahi, and M. G. Roozbahani, "Design of a band-notched microstrip circular slot antenna for UWB communication," *Progress In Electromagnetics Research C*, Vol. 12, 113–123, 2010.
24. Tu, S., Y.-C. Jiao, Y. Song, B. Yang, and X. Wang, "A novel monopole dual band-notched antenna with tapered slot for UWB applications," *Progress In Electromagnetics Research Letters*, Vol. 10, 49–57, 2009.
25. Wang, L., W. Wu, X.-W. Shi, F. Wei, and Q. Huang, "Design of a novel monopole UWB antenna with a notched ground," *Progress In Electromagnetics Research C*, Vol. 5, 13–20, 2008.
26. Lin, C.-C. and H.-R. Chuang, "A 3–12 GHz UWB planar triangular monopole antenna with ridged ground-plane," *Progress In Electromagnetics Research*, Vol. 83, 307–321, 2008.
27. Bates, R. N., "Design of microstrip spur-line band-stop filters," *Microwave, Optics and Acoustics*, Vol. 1, No. 6, 1977.
28. Computer Simulation Technology, CST studio suite 2010, www.cst.com.

29. Pancera, E., J. Timmermann, T. Zwick, and W. Wiesbeck, "Time domain analysis of band notch UWB antennas," *Proc. of European Conference on Antenna and Propagation*, 3658–3662, 2009.
30. Sheng, H., P. Orlik, A. M. Haimovich, L. J. Cimini, and J. Zhang, "On the spectral and power requirements for ultra-wideband transmission," *Proc. IEEE Int. Conf. Communications*, Vol. 1, 738–742, Anchorage, AL, 2003.
31. Kim, H., D. Park, and Y. Joo, "All-digital low-power CMOS pulse generator for UWB system," *Electron. Lett.*, Vol. 40, No. 24, 1534–1535, 2004.
32. Liang, J., C. C. Chiau, X. Chen, and C. G. Parini, "Study of a printed circular disc monopole antenna for UWB systems," *IEEE Trans. Antennas Propag.*, Vol. 53, No. 11, 3500–3504, 2005.
33. Yang, Y.-Y., Q.-X. Chu, and Z.-A. Zheng, "Time domain characteristics of band-notched ultrawideband antenna," *IEEE Trans. Antennas Propag.*, Vol. 57, No. 10, Oct. 2009.
34. Wu, Q., R.-H. Jin, and J.-P. Geng, "Pulse preserving capabilities of printed circular disk monopole antennas with different substrates," *Progress In Electromagnetics Research*, Vol. 78, 349–360, 2008.
35. Kwon, D.-H., "Effect of antenna gain and group delay variations on pulse-preserving capabilities of ultrawideband antennas," *IEEE Trans. Antennas Propag.*, Vol. 54, No. 8, Aug. 2006.